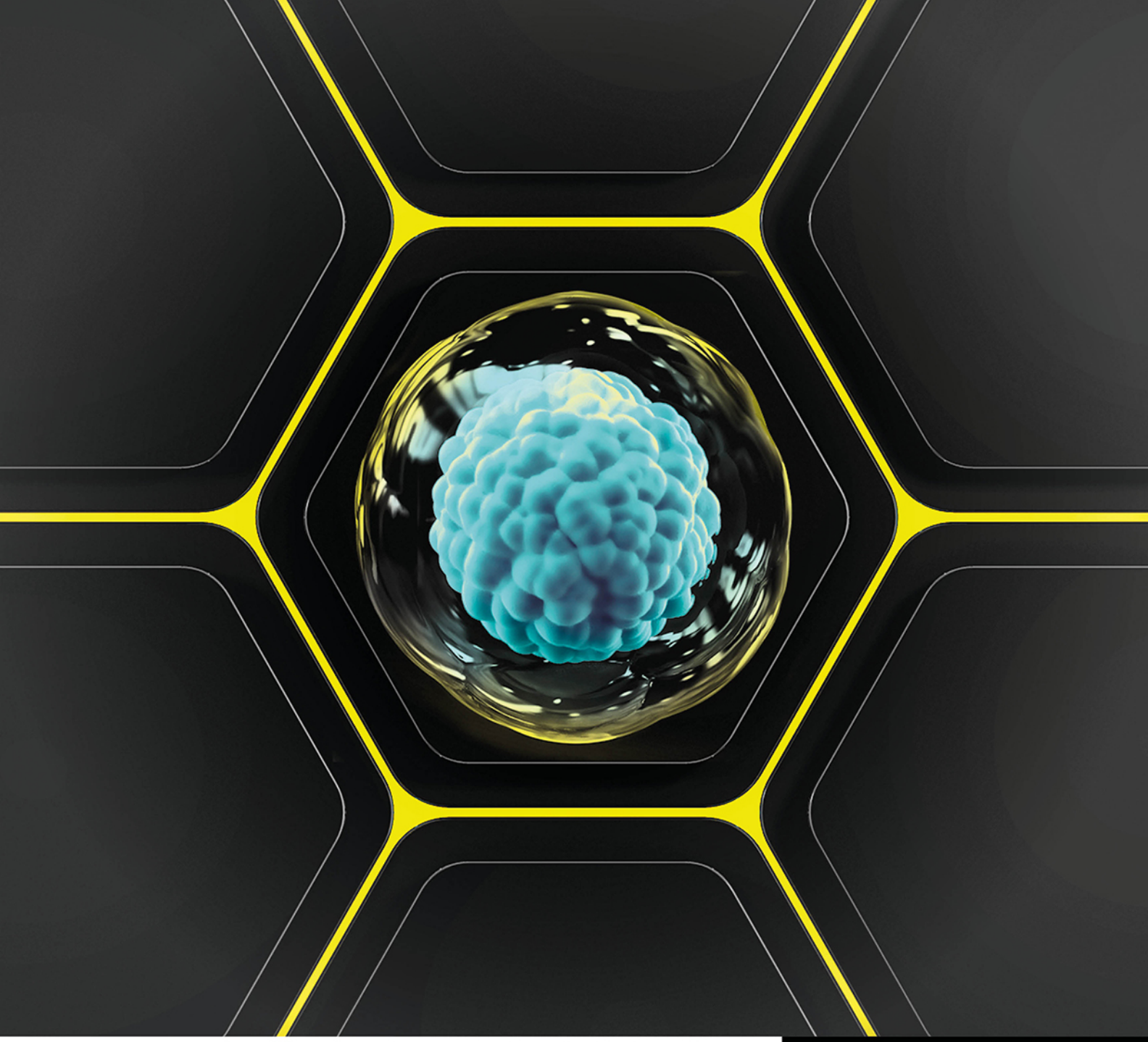

Transforming Liquid Biopsy Analysis

Simplifying Progress

Isolate pure single tumor cells from liquid biopsies with CellCelector Flex

Learn how CellCelector Flex can reduce steps, streamline workflows, and accelerate processing - while capturing cells without loss or damage, enabling high viability and up to 100% efficiency.

It's a unique and complete solution for detecting and isolating CTCs after enrichment and staining steps. In just 10 minutes, you can pick 20 individual CTCs for DNA, RNA or proteome analysis.

Learn more:
www.sartorius.com/cellcelector

SARTORIUS

ARTICLE

BIOTECHNOLOGY and BIOENGINEERING

A Cleavable Silica-Binding Affinity Tag for Rapid and Inexpensive Protein Purification

Brandon L. Coyle, François Baneyx

Department of Chemical Engineering, University of Washington, Box 351750, Seattle, Washington 98195-1750; telephone: 206-685-7659; fax: 206-685-3451; e-mail: baneyx@uw.edu

ABSTRACT: We describe a new affinity purification tag called Car9 that confers proteins to which it is fused micromolar affinity for unmodified silica. When appended to the C-terminus of GFPmut2 through a flexible linker, Car9 promotes efficient adsorption to silica gel and the fusion protein can be released from the particles by incubation with L-lysine. Using a silica gel column and the lysine elution approach in fast protein liquid chromatography (FPLC) mode, Car9-tagged versions of GFPmut2, mCherry and maltose binding protein (MBP) can be recovered from clarified lysates with a purity of 80–90%. Capitalizing on silica's ability to handle large pressure drops, we further show that it is possible to go from cell lysates to purified protein in less than 15 min using a fully disposable device. Finally, we demonstrate that the linker-Car9 region is susceptible to proteolysis by *E. coli* OmpT and take advantage of this observation to excise the C-terminal extension of GFPmut2-Car9 by incubating purified fusion protein with cells that overproduce the outer membrane protease OmpT. The set of strategies described herein, should reduce the cost of affinity purification by at least 10-fold, cut down purification times to minutes, and allow for the production of proteins with native (or nearly native) termini from their C-terminally-tagged versions.

Biotechnol. Bioeng. 2014;111: 2019–2026.

KEYWORDS: purification; affinity tag; fusion protein; silica; proteolytic cleavage

Introduction

Affinity tags have revolutionized protein purification by enabling one-step recovery of recombinant proteins from contaminating species. Tags are generally fused to the N- or C-terminus of expression targets and range in size from full-length proteins that bind with high affinity to immobilized substrates (e.g., maltose binding protein and glutathione S transferase) to short peptides recognized by immobilized antibodies or proteins (e.g., FLAG, c-myc, and Streptag) (Arnau et al., 2006; Waugh, 2005). By far, the most widely used affinity tag is the hexahistidine (His) extension, which confers high affinity for transition metal ions (e.g., Ni^{2+} and Co^{2+}) immobilized on a solid support through a coordinating ligand (e.g., nitrilotriacetate; NTA) (Kuo and Chase, 2011). While such resins are significantly cheaper than immobilized antibodies and proteins, they remain expensive. For example, the cost of purifying a His-tagged protein on Ni-NTA has been estimated to be $2 per mg of purified protein (Lichty et al., 2005).

Because purification costs are primarily associated with the price of the stationary phase, and to a lesser extent with that of the eluent, the development of affinity purification schemes relying on earth-abundant materials is desirable. One such material is silica gel, a porous and vitreous form of SiO_2, which has been extensively used as a chemically modifiable stationary phase for chromatography because it engenders low pressure drops and can be produced with controlled particle and pore sizes (Ghose et al., 2004). To date, however, few attempts have been made at using underivatized silica for protein purification.

Here, we show that Car9, a dodecapeptide that we previously identified for its ability to bind carbonaceous substrates (Coyle et al., 2013a), exhibits micromolar affinity for silica gel. By exploiting the fact that this interaction can be disrupted by L-lysine, we develop and validate a new affinity purification scheme that supports rapid and inexpensive protein purification. We also describe a companion strategy for cost-effective excision of Car9-based C-terminal tags.

Materials and Methods

DNA Manipulations and Protein Purification

Plasmid pBLN200, a pET-24a(+) (Novagen) derivative in which the T7 promoter has been replaced by a DNA segment encoding the *araC* gene and the arabinose-inducible P_{BAD}

The authors have filed for a patent and declare competing financial interest.
Correspondence to: F. Baneyx
Contract grant sponsor: Office of Naval Research
Contract grant number: BRC-11123566
Received 1 February 2014; Revision received 27 March 2014; Accepted 31 March 2014
Accepted manuscript online 28 April 2014;
Article first published online 4 June 2014 in Wiley Online Library (http://onlinelibrary.wiley.com/doi/10.1002/bit.25257/abstract).
DOI 10.1002/bit.25257

promoter was described elsewhere (Nannenga and Baneyx, 2011). Plasmid pBLN200-Car9 (Supplementary Fig. S1) was constructed by inserting a *Hin*dIII-*Xho*I cassette encoding a GGGS linker and the Car9 dodecamer into the same sites of pBLN200. Genes encoding GFPmut2, MBP and His6-mCherry were PCR-amplified on *Nde*I-*Hin*dIII fragments and inserted into the same sites of pBLN200-Car9. Derivatives of pBLN200 encoding the wild type proteins were also built. All DNA constructions and initial expression experiments were in Top10 cells (F^- *endA*1 *recA*1 *hsdR*17 (r_k^-, $m_k^+r^-{}_k$,$m^+{}_k$) λ^- *supE*44 *thi*1 *gyrA*96 *relA*1 ϕ80Δ*lac*Δ*M15*Δ (*lacZYA-argF*)U169 *deo*R). Plasmids were also introduced in *E. coli* KS272 (F′ Δ*lacX*74 *galE galK thi rps*L(*strA*) Δ*phoA*) (Strauch et al., 1989) and in SF100 (KS272 Δ*ompT*) (Baneyx and Georgiou, 1990). Seed cultures (25 mL) were used to inoculate 500 mL of LB medium supplemented with 50 μg/mL kanamycin and cells were grown to $A_{600} \approx 0.5$ at 37°C. Cultures were transferred to a 25°C water bath for 10 min and protein synthesis was induced by addition of 2% L-Arabinose. This expression temperature was selected for consistency with a previous study (Coyle et al., 2013a). After 6 h of cultivation, cells were harvested by centrifugation at 7,000*g* for 5 min, resuspended in 35 mL of 20 mM Tris–HCl pH 7.5 (Buffer A) supplemented with 2 mM EDTA, and disrupted by six rounds of sonication for 3 min at 30% duty cycle using a Branson sonifier. Lysates were clarified by centrifugation at 10,000*g* for 15 min. GFPmut2, MBP, and mCherry were purified to near homogeneity by ion exchange chromatography on a Whatman DE52 column. Typical protein concentration was 50 μM (0.67 mg/mL).

Characterization of Protein–Silica Interactions

The homemade Surface Plasmon Resonance (SPR) chips used in our experiments consisted of a glass substrate coated with a ≈2 nm titanium adhesion layer, a ≈48 nm evaporated gold film, and a ≈4 nm silicon film deposited by plasma enhanced chemical vapor deposition. Chips were cleaned by ethanol and UV-ozone treatment and mounted on a 4-channel flow cell SPR sensor from the Institute of Photonics and Electronics (Prague, Czech Republic). SPR experiments were conducted with purified TrxA, TrxA::Car9, GFPmut2 and GFPmut2-Car9 as previously described (Coyle et al., 2013a).

Silica gel (60-220 μm particles with 6 nm pores) was purchased from Sigma-Aldrich. For fluorescence depletion assays, the gel was washed several times with Buffer A to remove fines and the indicated amount of settled powder was transferred to pre-weighed PCR tubes. Proteins (150 μL from 2.5 μM stock solutions) were added and the mixtures were incubated for 1h at room temperature. Supernatants were removed and the fluorescence was quantified on a Hitachi F-4500 fluorescent spectrophotometer with excitation at 488 nm and emission slit width set at 2.5 nm. Protein concentrations were quantified using a calibration curve constructed with dilutions of GFPmut2 and GFPmut2-Car9, as appropriate.

Tag Cleavage by OmpT

For the experiments of Fig. 5A, cultures of Top10 cells harboring pBLN200-GFPmut2-Car9 were grown to $A_{600} \approx 0.5$ at 37°C in 25 mL of LB medium supplemented with 50 μg/mL kanamycin. Flasks were transferred to 25°C for 10 min and protein synthesis induced by addition of 2% L-Arabinose. After 6 h, samples (3 mL) were harvested by centrifugation at 7,000*g* for 5 min, resuspended in 5 mL of Buffer A supplemented with 2 mM EDTA, and disrupted by three rounds of French pressing. Lysates were separated into soluble and insoluble fractions by centrifugation at 10,000*g* for 15 min. Clarified lysates were kept on ice for 30 min and subjected to methanol/chloroform extraction as described (Wessel and Flügge, 1984). Proteins were resuspended in SDS loading buffer and samples corresponding to identical amounts of cells (Thomas and Baneyx, 1996) were fractionated by gel electrophoresis. For the experiments of Fig. 5B, KS272 or SF100 cells harboring pBLN200-Gfpmut2-Car9 were grown and lysed as above. Unbroken cells were removed by centrifugation at 10,000 *g* for 15 min, and lysates were incubated at 0°C or 25°C for 1h. Clarification and protein precipitation was performed as above.

For the tag removal experiments of Figure 6, SF100 cells transformed or not with pML19 were grown at 37°C in 25 mL LB medium supplemented with 100 μg/mL carbenicillin. After 5 h of growth at 37°C, cells were harvested from culture volumes corresponding to three absorbance units at 600 nm (A_{600}) and washed three times with 2 mL of 50 mM sodium phosphate pH 7.5 with intervening 5,000*g* centrifugation steps. After the final wash, cells were resuspended in 100 μL of 50 mM phosphate buffer pH 7.5 containing purified GFPmut2-Car9 at 10 μM final concentration. After 30 or 45 min incubation at room temperature, cells were sedimented at 5,000*g*, and aliquots of the supernatants were fractionated by SDS–PAGE.

Purification of Tagged Proteins on Silica Gel Columns

Silica gel (3 g) was washed thoroughly with Buffer A and the slurry was incubated with 5 mL of clarified cell lysate prepared as above. After overnight incubation at 8°C with gentle agitation, the gel was transferred to a 1 cm inner diameter chromatography column (GE Healthcare, Pittsburgh, PA) that was washed at 1 mL/min with buffer A until no protein was detected in the effluent (> 5 column volumes). Target proteins were eluted in ≈45 mL using the same flow rate of buffer A supplemented with 1 M L-lysine. Protein concentrations were determined using the BCA protein assay (Thermo Scientific, Rockford, IL) and bovine serum albumin as a standard. Protein purity was determined by videodensitometric analysis of SDS–PAGE minigels using the NIH Image J software. It is defined here as the ratio of target band intensity to sum of the intensities of all bands in a lane. Starting purity/expression levels for the experiments of Figure 4 were 12%, 28%, and 11% for GFPmut2-Car9, MBP-Car9, and mCherry-Car9, respectively.

Disposable Setup for Rapid Purification

Silica slurry (3 g; ≈5 mL) was loaded in the barrel of a 30 mL syringe that had been plugged with glass wool and connected to a second 30 mL syringe through a plastic two-way valve. A perforated plastic disc was placed on top of the bed to keep the stationary phase settled. Clarified lysate (5 mL) prepared as above, was dispensed on top of the bed, the valve was opened and the fluid was aspired at a flow rate of ≈30 mL/min. The time elapsed between dispensing the lysate and aspiration was less than 5 s. When the top of the bed was reached, the valve was closed and 30 mL of Buffer A was added to the top barrel and drawn through the bed as above. The wash process was repeated three times for a total wash volume of 90 mL (no protein could be detected at larger wash volumes). GFPmut2-Car9 was eluted with Buffer A supplemented with 1 M L-lysine. The first 5 mL (corresponding to wash buffer) were discarded and 60 mL of elution buffer were passed through. The protein was concentrated on a 10-kDa cutoff Amicon ultra centrifugal filters (Millipore).

Results and Discussion

Car9 Is as a Silica-Binding Peptide

Previously, we used the FliTrx cell surface display system (Lu et al., 1995) to identify disulfide-constrained dodecapeptides that discriminate between allotropes of carbon (Coyle et al., 2013a). One of these binders, called Car9 (amino acid sequence DSARGFKKPGKR using the one letter code), was found to bind to graphitic materials through a combination of electrostatic interactions (between basic K and R residues and negatively charged hydroxyl and carbonyl groups dangling from the materials' edges) and π–π interactions (between the F residue and the planar six-carbon rings of graphene-based materials) (Coyle et al., 2013a). Because silica (SiO_2) surfaces are rich in hydroxyl-terminated silanol groups (Fig. 1A), we hypothesized that Car9 may also function as a silica binder. As an initial test of this idea, we conducted surface plasmon resonance (SPR) experiments using TrxA::Car9, a derivative of *E. coli* thioredoxin 1 (TrxA) that specifies a disulfide-constrained Car9 sequence flanked by CGP and GCP tripeptides in place of the protein's native CGPC active site. The fusion protein along with wild type TrxA were expressed and purified as described (Coyle et al., 2013a) and chemical vapor deposition was used to coat the surface of SPR chips with a thin film of silicon that spontaneously develops an SiO_2 layer upon exposure to atmospheric oxygen (Iler, 1979). SPR experiments conducted at a protein concentration of 1 μM revealed that TrxA::Car9 adsorbed to these chips with rapid kinetics (Fig. 1B, squares) and that more than half of this material was retained when the chip was washed with buffer to remove loosely bound material (arrow). By contrast, wild type TrxA did not appreciably bind to silica (Fig. 1B, circles), unambiguously establishing that disulfide-constrained Car9 is a silica binding peptide in addition to being a carbon binder.

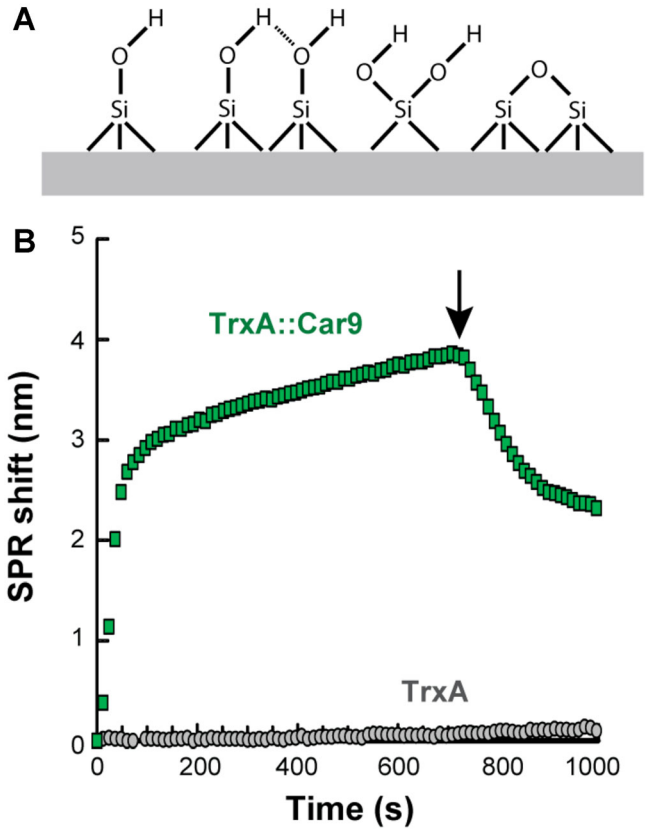

Figure 1. Disulfide-constrained Car9 tag binds to silica. **A**: Surface chemistry of silica. From left to right: free silanol, hydrogen-bonded silanol, germinal silanol, and siloxane. **B**: Surface plasmon resonance (SPR) sensogram of the adsorption of wild type TrxA and TrxA::Car9 on silica chips at 1 μM concentration. The arrow indicates the start of the wash step.

A Linear Version of Car9 Endows GFP With Silica-Binding Ability

Conversion of solid binding peptides from a disulfide-constrained to a linear conformation can affect their ability to bind to their cognate solids and modulate their ability to control the nucleation and growth of inorganic phases (Chen et al., 2009; Chiu et al., 2012; Choe et al., 2007; Coyle et al., 2013a; Hnilova et al., 2008; Seker et al., 2007). To determine if presentation in a disulfide-bonded loop is required for Car9 to bind silica and to facilitate the construction of fusion proteins containing a C-terminal Car9 extension, we inserted a DNA cassette specifying a flexible GGGS linker and the Car9 dodecamer downstream of the arabinose-inducible P_{BAD} promoter in pBLN200 (Nannenga and Baneyx, 2011) (Supplementary Fig. S1). Using this system, we appended Car9 to GFPmut2, an improved folding

mutant of *A. victoria* GFP containing the S65A, V68L, and S72A substitutions (Cormack et al., 1996), and purified wild type and tagged proteins by conventional ion exchange chromatography. As expected from the charged and hydrophilic nature of the tag and the fact that it is separated from its fusion partner by a flexible linker, Car9 had no deleterious effect on the optical properties of GFPmut2 (Supplementary Fig. S2).

We next constructed Langmuir adsorption isotherms using silica-coated SPR chips and increasing concentrations of purified GFPmut2-Car9 or GFPmut2. Figure 2 shows that while the parental protein had little affinity for silica (circles), GFPmut2-Car9 bound to the SiO_2 surface in a concentration dependent manner and with a calculated equilibrium dissociation constant (K_d) of 1 μM (squares). This value is identical to that reported for the interaction of His-tagged proteins and Ni-NTA-coated surfaces (Nieba et al., 1997).

To confirm the above results with a form of silica that is relevant to chromatography, a constant amount of GFPmut2-Car9 or GFPmut2 (10 μg) was incubated with increasing loads of silica gel for 1h at room temperature and the fluorescence remaining in the supernatant was quantified by spectroscopy. GFPmut2-Car9 progressively partitioned in the solid phase (Fig. 3A) and nearly all of the fluorescent material was depleted from the supernatant in the presence of ≈35 mg silica gel (Fig. 3C, squares). By contrast, GFPmut2 adsorbed nonspecifically to the matrix and the majority of the untagged protein remained in the supernatant even when we added 5 times the amount of silica gel needed to quantitatively pull down GFPmut2-Car9 (Fig. 3B and C, circles). In summary, linear Car9 is fully functional for binding to silica gel and it does so with an affinity and capacity suitable for the development of chromatography schemes.

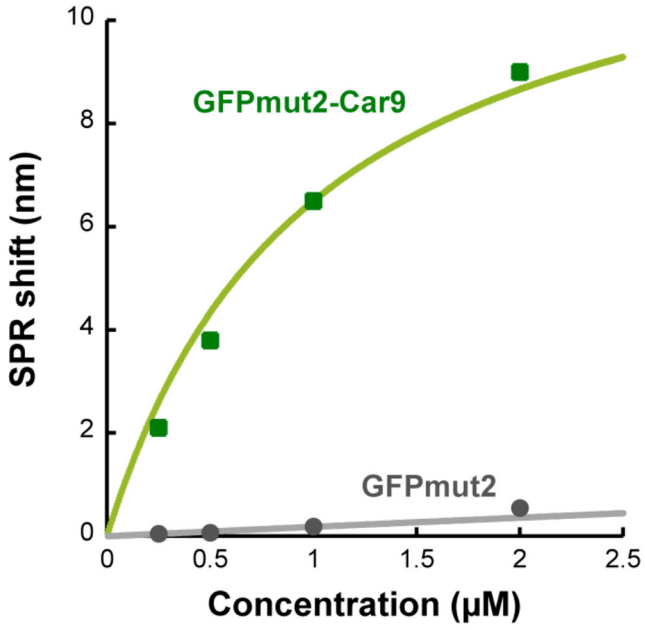

Figure 2. Langmuir adsorption isotherms of purified GFPmut2-Car9 and GFPmut2 on silica as determined by SPR experiments conducted at the indicated protein concentrations.

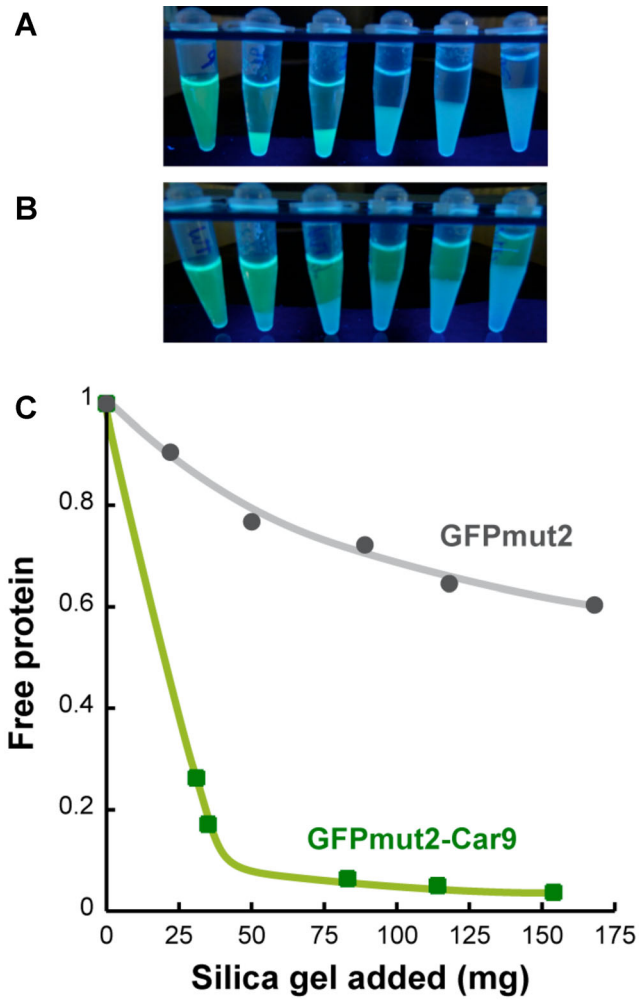

Figure 3. Adsorption of GFPmut2 and GFPmut2-Car9 to silica gel. **A**: GFPmut2-Car9 (2.5 μM) was incubated with increasing amounts of silica and tubes were photographed under UV light. **B**: As in panel A using 2.5 μM GFPmut2. **C**: The binding of GFPmut2 and GFPmut2-Car9 to silica gel was quantified by measuring the fluorescence remaining in the supernatant. Fluorescence is normalized to an arbitrary value of 1 in the absence of silica.

L-Lysine Is an Effective Eluent for Releasing Car9 Fusions From Silica Gel

Easy removal of proteins from the stationary phases to which they selectively adsorb is a prerequisite for the development of useful purification schemes. We therefore tested a number of conditions to elute GFPmut2-Car9 from silica gel. Although the tag contains five basic residues, neither high

ionic strength buffers (5 M NaCl or 5 M $MgCl_2$), nor alkaline solutions (up to pH 10) proved effective at releasing the protein. Taken together with other studies (Patwardhan et al., 2012; Stutz, 2009), these results suggest that the binding of Car9 to silica not only involves electrostatic interactions between basic residues and silanol groups but also hydrophobic contacts between the central phenylalanine and siloxane groups (Fig. 1A).

We reasoned that because Car9 specifies four lysines (a positively-charged residue whose side chain has a hydrophobic character), the free amino acid might prove useful as a competitive eluent. Indeed, incubation of silica-bound GFPmut2-Car9 with a solution of 1 M L-lysine led to efficient release of functional (fluorescent) protein from the particles (Fig. 4A).

To validate this strategy, clarified extracts from SF100 (Δ*ompT*; see below) cells expressing GFPmut2-Car9 were incubated with silica gel and loaded on a FPLC column that was washed at 1 mL/min with buffer to remove contaminants. Addition of 1 M L-lysine to the buffer led to efficient elution of GFPmut2-Car9 with a purity of ≈80% (Fig. 4B). To demonstrate broad applicability, we fused the Car9 tag to the C-termini of MBP and mCherry (a monomeric derivative of *Dicosoma* sp. DsRed) (Shaner et al., 2004) and repeated the above experiment. These two targets could be recovered with ≈90% and 80% purity with no attempt at optimizing loading or elution conditions.

From the above experiments, we estimate that the binding capacity of silica for Car9-tagged proteins is ≈4 mg per mL of settled slurry. This is comparable to the capacity of Ni-NTA for His-tagged proteins (5–10 mg per mL) and that of cross-linked amylose for MBP (7–10 mg per mL).

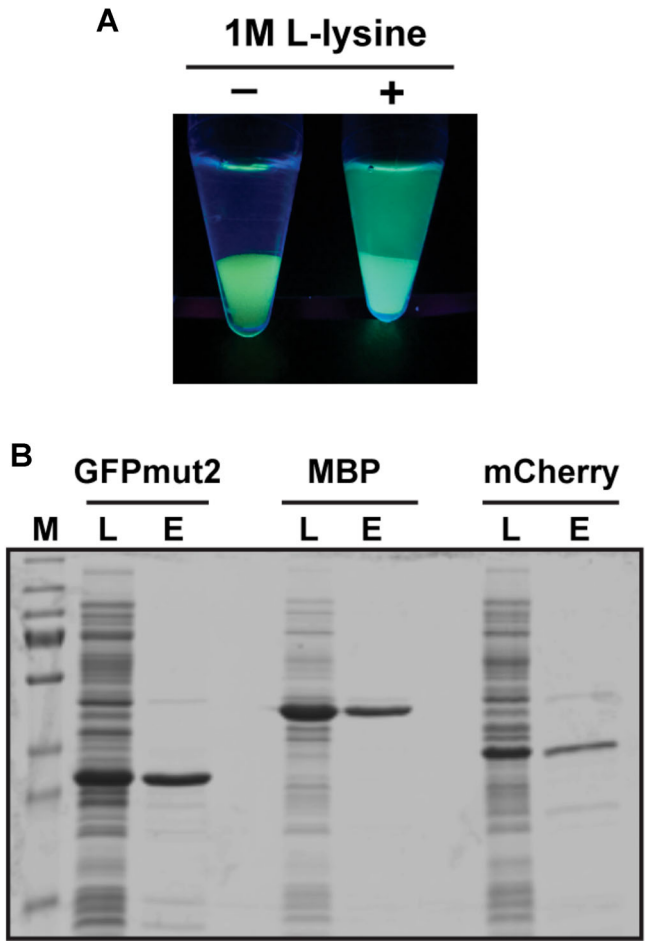

Figure 4. Eluting Car9-tagged proteins with L-lysine. **A**: Release of GFPmut2-Car9 from silica gel upon incubation with 1 M L-lysine. **B**: SDS–PAGE analysis of clarified lysates (L) and lysine-eluted (E) fractions from cells producing GFPmut2-Car9, MBP-Car9, and mCherry-Car9

The Car9 Tag is Cleaved by Outer Membrane Protease OmpT

During initial expression and purification experiments in Top10 cells, we noticed the appearance of two large degradation fragments of GFPmut2-Car9 in soluble cell extracts that had been held on ice (Fig. 5A, lane S, black arrows). There was no degradation of wild type GFPmut2 under the same conditions (Supplementary Fig. S3) and GFPmut2-Car9 remained intact in undisrupted cells or when deposited into inclusion bodies (Fig. 5A, lanes WC and I, respectively). These results suggested that a cell envelope-associated protease was recognizing the tag at two different positions. Because fusion of the linker-Car9 region to GFPmut2 introduces a Lys–Lys dipeptide at the fusion joint, and because the tag itself contains an internal Lys–Lys as well as a C-terminal Lys–Arg sequence (Fig. 5C), we suspected the involvement of OmpT, an aspartate outer membrane protease specific for paired basic residues (Sugimura and Nishihara, 1988). To test this hypothesis, we introduced the plasmid encoding GFPmut2-Car9 into KS272 and SF100, two isogenic strains containing intact and null *ompT* alleles, respectively. As expected, extracts of $ompT^{+}$ cells contained the two degradation products after 1 h incubation on ice (Fig. 5B, black arrows). Furthermore, conversion of the high molecular mass degradation product into a smaller species that was unable to bind silica (Supplementary Fig. S4) was accelerated when extracts were held at 25°C. By contrast, there was no detectable proteolysis of GFPmut2-Car9 when extracts of Δ*ompT* (SF100) cells were incubated at the same temperature (Fig. 5B), firmly establishing OmpT as the protease responsible for the cleavage of the Car9 extension.

Removing the Affinity Tag With Whole Cells That Overexpress OmpT

The removal of affinity tags might be desirable if they interfere with biological function or contribute to immunogenicity. This is generally accomplished by engineering the recognition sequence of an endoprotease between affinity tag and fusion partner and making use of the corresponding immobilized or affinity-tagged protease to cleave off the

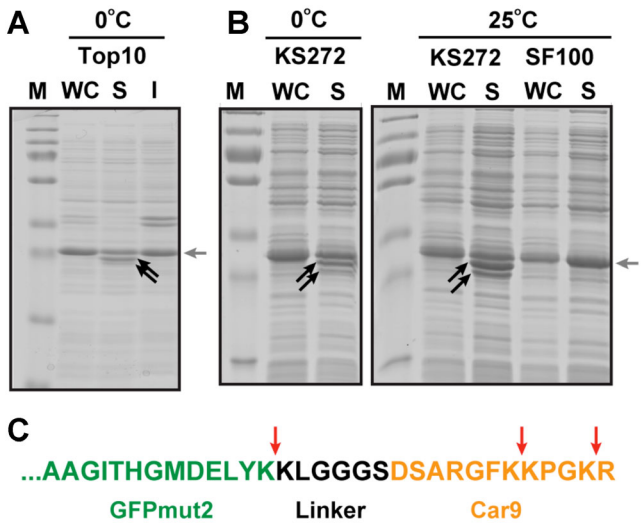

Figure 5. The linker-Car9 extension is susceptible to cleavage by OmpT. **A**: Top10 (*ompT*$^+$) cells expressing GFPmut2-Car9 were left unbroken (WC) or disrupted by sonication and centrifuged at 10000g to produce soluble (S) and insoluble (I) fractions. Gray arrows show the migration position of intact GFPmut2-Car9, black arrows that of the degradation products. **B**: KS272 (*ompT*$^+$) or SF100 (Δ*ompT*) cells expressing GFPmut2-Car9 were left unbroken (WC) or disrupted by sonication and subjected to centrifugation to produce soluble (S) fractions. Proteins were fractionated after 1h incubation at 0 or 25°C, as indicated. **C**) Amino acid sequence of the C-terminus of GFPmut2-Car9. Regions corresponding to wild type GFPmut2, linker and Car9 sequence are colored and labeled. Arrows show the position of OmpT cleavage sites.

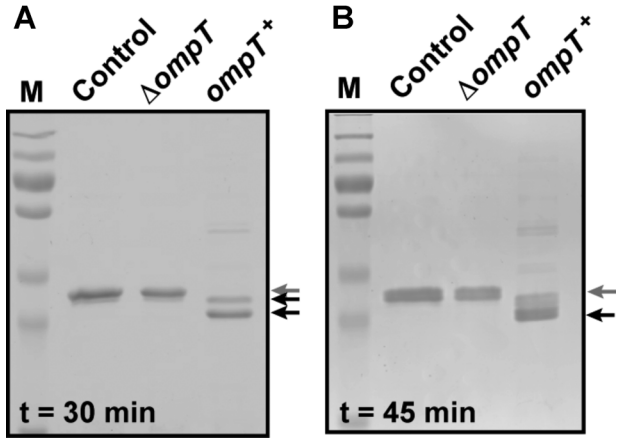

Figure 6. Cleaving the linker-Car9 extension of GFPmut2-Car9 with OmpT-producing cells. Purified GFPmut2-Car9 (Control) was incubated with whole cells lacking (Δ*ompT*) or overproducing OmpT (*ompT*$^+$). Soluble proteins were subjected to SDS-PAGE after 30 or 45 min of incubation and removal of the cells.

extension (Waugh, 2011). While proteases such as thrombin, tobacco etch virus (TEV) protease and enteropeptidase produce nearly native products when their recognition sequence is inserted between a N-terminal affinity tag and the N-terminus of a target protein, they are not as useful for precise excision of C-terminal affinity tags owing to the fact that protease specificity determinants are located on the N-terminal side of the cleavage site (Waugh, 2011).

The involvement of OmpT in the processing of the linker-Car9 extension suggested that this protease might be useful within the context of intact cells to inexpensively remove the affinity tag and yield a protein with a single extra basic amino acid (and, in the special case of GFPmut2, a native C-terminus; Fig. 5C). To test this idea, SF100 cells transformed or not with pML19 (a pUC derivative that encodes OmpT; (Gayda and Markovitz, 1978; Grodberg and Dunn, 1988) were incubated at room temperature with purified GFPmut2-Car9 as described in Materials and Methods. Cells were sedimented by low speed centrifugation and aliquots of the supernatants were subjected to electrophoresis. Figure 6 shows that while the fusion protein remained intact when placed in contact with Δ*ompT* cells (gray arrows), it was converted into its expected degradation products after 30 min of incubation with OmpT-overproducing cells. In addition, tag-free GFPmut2 was the dominant product after 15 additional minutes of incubation (bottom arrow). The samples also contained a small amount of high molecular weight contaminants that were not seen when incubation was conducted with Δ*ompT* cells. These bands likely correspond to host proteins released from SF100 cells that are fragilized or lysed due to OmpT overproduction. The problem should be easy to address by using a different strain and/or adjusting incubation time and temperature.

Overall, our results indicate that the C-terminal linker-Car9 extension is accessible to OmpT and that cells expressing this protease on their surface can be used as an inexpensive reagent to cleave linker and affinity tag.

Rapid and Inexpensive Purification of Car9-Tagged Proteins

Silica matrices tolerate high-pressure drops and have been used for ultrafast (*a.k.a.* Flash) purification of organic species using a scheme in which the mobile phase is driven at high flow rate through the column by applied air pressure (Still et al., 1978). To determine if a similar approach could be used for the rapid purification of Car9-tagged proteins using a disposable setup, we connected two plastic syringes to a control valve and placed washed silica gel above glass wool in the top barrel (Fig. 7A). We next dispensed clarified extract from GFPmut-Car9 producing cells, immediately aspired it through the bed by pulling the piston of the bottom syringe and washed the gel with buffer as detailed in Materials and Methods. Finally, we eluted bound protein by vacuum aspiration of buffer supplemented with L-lysine. This procedure yielded 85% pure GFPmut-Car9 (Fig. 7B). Remarkably, by performing all fluid handling steps at a flow rate of ≈30 mL/min, it was possible to go from clarified extract to pure protein (≈0.5 mg/mL) in less than 15 min.

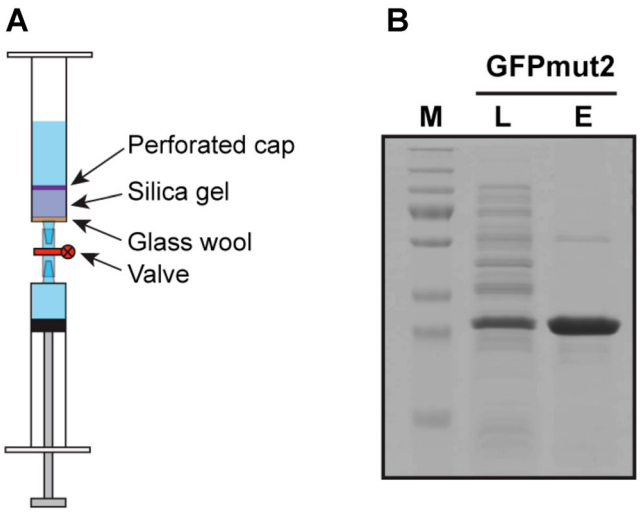

Figure 7. Rapid purification of Car9-tagged proteins with a disposable device. **A**: Schematic representation of the device. **B**: SDS–PAGE analysis of clarified lysate from cells producing GFPmut2-Car9 before loading (L) and after lysine elution (E).

Finally, we compared the cost of purifying a Car9-tagged protein on a disposable silica gel column to that of purifying a His-tagged protein on a reusable Ni-NTA column of comparable volume. This calculation revealed that even when the cost of the more expensive lysine elution buffer is factored in, it would take at least 15 reuses of the Ni-NTA resin to break even with the cost of the Car9 tag/disposable silica gel technology (Supplementary Table S1).

Conclusion

From DNA miniprep kits to next-generation sequencing, rapid and inexpensive methods that simplify formerly complex tasks have revolutionized the practice of life sciences. Protein purification is only halfway there: although affinity tags (Arnau et al., 2006; Waugh, 2005) have transformed what used to be a time-consuming series of chromatography steps into a single-stage process (albeit with some loss of purity), affinity purification remains expensive. Here, we described and validated a new affinity tag and elution conditions for protein purification on unmodified silica. We further demonstrated a disposable companion system that allows for the purification of Car9-tagged proteins from crude cell extracts in a matter of minutes and for less than $2 per run under worst-case scenario conditions. Finally, we showed that the susceptibility of the linker-Car9 region to proteolysis by outer membrane protease OmpT can be exploited to remove the C-terminal extension.

In addition to enabling rapid protein purification at the lab scale and inexpensive protein production at the large scale, we anticipate that the strategy described herein will prove useful for multiplex protein purification using vacuum manifolds. The use of OmpT-overproducing cells to remove Car9 extensions should be applicable to other targets. For C-terminal tags, this operation will yield proteins terminated with a lysine or arginine residue, but free of the longer extensions generated by other endoproteases. Clearly, the success of the approach will depend on the absence of other accessible OmpT sites on the target protein.

Even though we have yet to optimize the system, we estimate that the Car9-tag/silica/lysine approach is at least 10-times cheaper than the use of His-tag/Ni-NTA/imidazole. The availability of such a low-cost purification technique should be instrumental in ushering a new era of green manufacturing where functional hybrid materials and systems are fabricated with proteins (Coyle et al., 2013b).

This work was supported by the Office of Naval Research through award BRC-11123566.

References

Arnau J, Lauritzen C, Petersen GE, Pedersen J. 2006. Current strategies for the use of affinity tags and tag removal for the purification of recombinant proteins. Protein Expr Purif 48:1–13.

Baneyx F, Georgiou G. 1990. In vivo degradation of secreted fusion proteins by the *Escherichia coli* outer membrane protein OmpT. J Bacteriol 172:494–494.

Chen HB, Su XD, Neoh K-G, Choe WS. 2009. Context-dependent adsorption behavior of cyclic and linear peptides on metal oxide. Langmuir 25:1588–1593.

Chiu D, Zhou W, Kitayaporn S, Schwartz DT, Murali-Krishna K, Kavanagh TJ, Baneyx F. 2012. Biomineralization and size control of calcium phosphate core-protein shell nanoparticles: Potential for vaccine applications. Bioconjug Chem 23:610–617.

Choe WS, Sastry MSR, Thai CK, Dai H, Schwartz DT, Baneyx F. 2007. Conformational control of inorganic adhesion in a designer protein engineered for cuprous oxide binding. Langmuir 23:11347–11350.

Cormack BP, Valdivia RH, Falkow S. 1996. FACS-optimized mutants of the green fluorescent protein (GFP). Gene 173:33–38.

Coyle BL, Rolandi M, Baneyx F. 2013a. Carbon-binding designer proteins that discriminate between sp2- and sp3-hybridized carbon surfaces. Langmuir 29:4839–4846.

Coyle BL, Zhou W, Baneyx F. 2013b. Protein-aided mineralization of inorganic nanostructures. In: Rehm BHA, editor. Bionanotechnology: Biological self-assembly and its applications. Norwich, UK: Caister Academic Press.

Gayda RC, Markovitz A. 1978. Cloned DNA fragment specifying major outer membrane protein a in *Escherichia coli* K-12. J Bacteriol 136(1):369–380.

Ghose S, McNemey TM, Hubbard B. 2004. Preparative protein purification on underivatized silica. Biotechnol Bioeng 87:413–423.

Grodberg J, Dunn JJ. 1988. ompT encodes the *Escherichia coli* outer membrane protease that cleaves T7 RNA polymerase during purification. J Bacteriol 170(3):1245–1253.

Hnilova M, Oren EE, Seker UOS, Wilson BR, Collino S, Evans JS, Tamerler C, Sarikaya M. 2008. Effect of molecular conformations on the adsorption behavior of gold-binding peptides. Langmuir 24:12440–12445.

Iler RK. 1979. The chemistry of silica: Solubility, polymerization, colloid and surface properties and biochemistry. New York, NY: Wiley.

Kuo WH, Chase HA. 2011. Exploiting the interactions between poly-histidine fusion tags and immobilized metal ions. Biotechnol Lett 33(6): 1075–1084.

Lichty JJ, Malecki JL, Michelson-Horowitz DJ, Tan S. 2005. Comparison of affinity tags for protein purification. Protein Expr Purif 41:98–105.

Lu Z, Murray KS, Van Cleave V, LaVallie ER, Stahl ML, McCoy JM. 1995. Expression of thioredoxin random peptide libraries on the *Escherichia coli* cell surface as functional fusions to flagellin: A system designed for exploring protein-protein interactions. Biotechnology 13:366–372.

Nannenga BL, Baneyx F. 2011. Reprogramming chaperone pathways to improve membrane protein expression in *Escherichia coli*. Protein Sci 20:1411–1420.

Nieba L, Nieba-Axmann E, Persson A, Hämäläinen M, Edebratt F, Hansson A, Lidholm J, Magnusson K, Karlsson AF, Plückthun A. 1997. BIACORE analysis of histidine-tagged proteins using a chelating NTA sensor chip. Anal Biochem 252:217–228.

Patwardhan SV, Emami FS, Berry RJ, Jones SE, Naik RR, Deschaume O, Heinz H, Perry CC. 2012. Chemistry of aqueous silica nanoparticle surfaces and the mechanism of selective peptide adsorption. J Am Chem Soc 134:6244–6256.

Seker UOS, Wilson B, Dincer S, Kim IW, Oren EE, Evans JS, Tamerler C, Sarikaya M. 2007. Adsorption behavior of linear and cyclic genetically engineered platinum binding peptides. Langmuir 23:7895–7900.

Shaner NC, Campbell RE, Steinbach PA, Giepmans BNG, Palmer AE, Tsien RY. 2004. Improved monomeric red, orange and yellow fluorescent proteins derived from *Discosoma* sp. red fluorescent protein. Nat Biotechnol 22:1567–1572.

Still WC, Kahn M, Mitra A. 1978. Rapid chromatography technique for preparative separations with moderate resolution. J Org Chem 43:2923–2925.

Strauch KM, Johnson K, Beckwith J. 1989. Characterization of *degP*, a gene required for proteolysis in the cell envelope and essential for growth of *Escherichia coli* at high temperature. J Bacteriol 171:2689–2696.

Stutz H. 2009. Protein attachment on silica surfaces—A survey of molecular fundamentals, resulting effects and novel preventive strategies in CE. Electrophoresis 30:2032–2061.

Sugimura K, Nishihara T. 1988. Purification, characterization, and primary structure of *Escherichia coli* protease VII with specificity for paired basic residues: Identity of protease VII and OmpT. J Bacteriol 170:5625–5632.

Thomas JG, Baneyx F. 1996. Protein misfolding and inclusion body formation in recombinant *Escherichia coli* cells overproducing heat-shock proteins. J Biol Chem 271:11141–11147.

Waugh DS. 2005. Making the most of affinity tags. Trends Biotechnol 23:316–320.

Waugh DS. 2011. An overview of enzymatic reagents for the removal of affinity tags. Protein Expr Purif 80:283–293.

Wessel D, Flügge UI. 1984. A method for the quantitative recovery of protein in dilute solution in the presence of detergents and lipids. Anal Biochem. 138:141–143.

Supporting Information

Additional Supporting Information may be found in the online version of this article at the publisher's web-site.